Adenosine 5′-triphosphate consumption by smooth muscle as predicted by the coupled four-state crossbridge model

Chi-Ming Hai* and Richard A. Murphy‡
*Section of Physiology and Biophysics, Division of Biology and Medicine, Brown University, Providence, Rhode Island 02912; and
‡Department of Physiology, School of Medicine, University of Virginia, Charlottesville, Virginia 22908

ABSTRACT We have proposed a four-state crossbridge model to explain contraction and the latch state in arterial smooth muscle. Ca^{2+}-dependent crossbridge phosphorylation was the only postulated regulatory mechanism and the latchbridge (a dephosphorylated, attached crossbridge) was the only novel element in the model. In this study, we used the model to predict rates of ATP consumption by crossbridge phosphorylation (J_{Phos}) and cycling (J_{Cycle}) during isometric and isotonic contractions in arterial smooth muscle; then we compared model predictions with experimental data. The model predicted that J_{Phos} and J_{Cycle} were similar in magnitude in isometric contractions, and both increased almost linearly with myosin phosphorylation. The predicted relationship between isometric stress and ATP consumption was quasihyperbolic, but approximately linear when myosin phosphorylation was below 35%, in agreement with most of the available data. Muscle shortening increased the predicted values of J_{Cycle} up to 3.7-fold depending on shortening velocity and the level of myosin phosphorylation. The predicted maximum work output per ATP was 7.4–7.8 kJ/mol ATP and was relatively insensitive to changes in myosin phosphorylation. The predicted increase in J_{Cycle} with shortening was in agreement with available data, but the model prediction that work output per ATP was insensitive to changes in myosin phosphorylation was unexpected and remains to be tested in future experiments.

INTRODUCTION

Crossbridge cycling rates as well as the number of attached crossbridges are regulated in smooth muscle (1). Isometric stress (an index of crossbridge attachment) and isotonic shortening velocity at low or zero load (an index of crossbridge cycling rates) increase together at the beginning of a contraction. However, shortening velocity subsequently falls during steady-state stress maintenance (the latch state: 2–4), which is also associated with a decrease in the rate of ATP consumption (5–9).

We have proposed a four-state crossbridge model (Fig. 1) to explain contraction and the latch state in the swine carotid media (10, 11). Ca^{2+}-calmodulin–dependent activation of myosin light chain kinase (12) was the only postulated regulatory mechanism, and the latchbridge (a dephosphorylated, attached crossbridge) was the only novel element in the model. The four-state model can quantitatively predict the following data sets in the swine carotid media: (*a*) time courses of myosin phosphorylation and isometric stress during contraction (10) and relaxation (13) and (*b*) quasihyperbolic dependence of steady-state isometric stress on myosin phosphorylation (14). The four-state model coupled to Huxley's model of strain-dependent cycling rates (coupled four-state model) can also explain variable stress–velocity relationships as a function of myosin phosphorylation (15). However, the four-state model has been criticized recently for an apparent failure to predict key energetic properties of smooth muscle, including the linear dependence of ATP consumption on isometric stress and the efficiency of contraction (16). Our goal in this study was to test the model further. To do so, we computed the predicted rates of ATP consumption by crossbridge phosphorylation (J_{Phos}) and cycling (J_{Cycle}) during isometric and isotonic contractions in the swine carotid media by coupling the four-state model with Huxley's concept of strain-dependent crossbridge cycling rates (17) and then compared model predictions with experimental data.

Address correspondence to Dr. Hai.

METHODS

The differential equations for solving the fraction of attached crossbridges (n) at a given crossbridge position (x) during isometric contraction and isovelocity shortening were solved analytically. When shortening velocity (dx/dt) was zero or constant, the system of time- and space-dependent partial differential equations was reduced to a system of space-dependent ordinary differential equations. The differential equations were then solved together with the algebraic equations for the strain-dependent crossbridge cycling rate constants. Numerical solutions were calculated using a FORTRAN program. The program was linked to the IMSL Math/PC-Library and run on an Intel 80286 microprocessor-based computer equipped with an Intel 80287 math co-processor. A variation of Newton's method was used to find the zero root of a nonlinear algebraic equation (18). As expected, the rate of crossbridges entering the crossbridge cycle should be the same as the rate of crossbridges leaving the crossbridge cycle during

0006-3495/91/02/530/12 $2.00

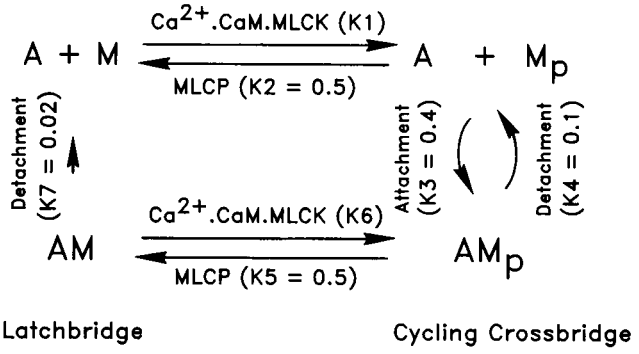

FIGURE 1 The four-state model. *A*, actin (thin filament); myosin crossbridge states are *M*, detached, dephosphorylated; *Mp*, detached, phosphorylated; *AMp*, attached, phosphorylated; *AM*, attached, dephosphorylated (latchbridge). *K1–K7* are first-order rate constants resolved from experimental data obtained from the swine carotid media (10, 14). *K1* and *K6* represent Ca^{2+}, calmodulin (*CaM*)-dependent myosin light chain kinase (*MLCK*) activity; *K2* and *K5* represent myosin light chain phosphatase (*MLCP*) activity. *K3* and *K4* represent attachment and detachment of phosphorylated crossbridges, and *K7* represents latchbridge detachment.

steady-state isometric contraction and isovelocity shortening. This served as a check of accuracy for the computer program. We compared fluxes of crossbridge attachment and detachment at different steady-states, and they were identical to the fourth significant figure.

RESULTS

We (19) and Paul (16) have calculated kinetic fluxes (content × rate constant) along the pathways in the four-state model (Fig. 1) and considered kinetic fluxes as rates of ATP consumption on the basis of the rationale that one molecule of ATP was consumed for each phosphorylation and crossbridge cycle during steady-state isometric contractions. However, ATP consumption by crossbridge cycling during isotonic contraction cannot be calculated by kinetic flux analysis because the kinetic model does not incorporate the strain and stress dependence of crossbridge cycling. Kinetic flux analysis may also be insufficient for calculating J_{Cycle} during isometric contraction for the following reasons. First, isometric stress is maintained by a population of crossbridges oriented in different positions relative to their equilibrium position and cycling at different rates (17, 20). Therefore, the apparent cycling rate constants derived from the time course of isometric stress development represent only the average behavior of the crossbridge population in a smooth muscle. Second, a free crossbridge can move randomly about its equilibrium position up to its maximum point of extension. The range of crossbridge movement can cover more than one crossbridge binding site on an actin filament. Therefore, statistically a crossbridge can interact with more than one binding site on an actin filament during its random movement. Huxley (17) modeled the strain dependence of crossbridge cycling rates and calculated J_{Cycle} during isometric and isotonic contractions by integrating the frequency of interaction between myosin crossbridges and an actin filament at all crossbridge positions. In this study we coupled Huxley's approach with the four-state model to compute J_{Cycle} during isometric and isotonic contractions.

We adapted Huxley's approach in modeling the strain dependence of the attachment (f) and detachment (g) rate constants of a crossbridge. Accordingly, we defined three regions of x where crossbridges cycle with different characteristics. When a crossbridge is located at the negative force–bearing region ($x < 0$), it cannot attach to an actin filament ($f = 0$) and detaches at a constant rate ($g = g_2$) independent of x within the boundary condition $x < 0$. However, when a crossbridge is located at the positive force–bearing region within its maximum extension (h) ($0 \leq x \leq h$), it cycles with f and g proportional to x ($f = f_1 x/h$ and $g = g_1 x/h$, where f_1 and g_1 are constants). Finally, when a crossbridge is located at the positive force–bearing region ($x \geq 0$) but beyond its maximum extension ($x \geq h$), it can only detach from the actin filament, and g is proportional to x ($f = 0$ and $g = g_1 x/h$; g_1 is the same constant as defined before). A linear dependence of f and g on x was the simplest model of strain-dependent crossbridge cycling rates. Since little is known about the behavior of single crossbridges in smooth muscle, we chose the simplest relationship to minimize the number of adjustable parameters in the model.

The strain-dependent cycling rate constants, f and g, are different from the apparent cycling rate constants resolved from the time course of isometric stress development. According to Huxley (17), the cycling rate constants f and g at $x = h$ (f_1 and g_1) were faster than any mechanical transients of a muscle, but f and g at $x = 0$ were 0. Fig. 2 shows the model's simulation of the time courses of crossbridge attachment at different x. As expected, f increased as x approached h. Since isometric stress represents the total number of attached crossbridges at all crossbridge positions between $x = 0$ and $x = h$, the apparent cycling rate constants derived from the rate of isometric stress development must be lower then f and g at $x = h$ but higher than f and g at $x = 0$. Since intracellular [Ca^{+2}] did not increase in a step in intact cells, and the presence of series elastic element further delayed stress development, we (15) previously estimated that the apparent attachment and detachment rate constants, $f(K)$ and $g(K)$, equaled $f_1/4$ and $g_1/4$, respectively. $f(K)$ was defined as the ratio of total flux of crossbridge attachment (as measured by isometric stress)

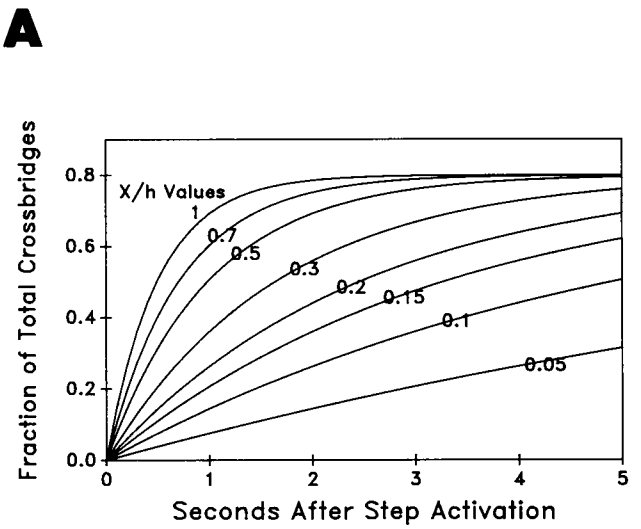

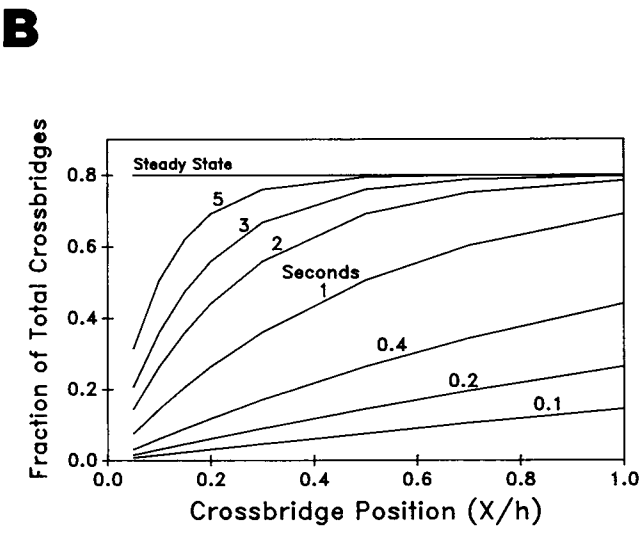

FIGURE 2 (*A*) Time courses of crossbridge attachment at different crossbridge positions (x/h) as predicted by the strain-dependent attachment (f) and detachment (g) rate constants. (*B*) Crossbridge attachment at different crossbridge positions (x/h) in the steady-state and at 0.1, 0.2, 0.4, 1, 2, 3, and 5 s after a step activation. In these simulations, $f = 1.6x/h$ and $g = 0.4x/h$ in s^{-1}, where h is the maximum extension of a crossbridge. Note that all model predictions yield smooth curves that are approximated by a series of straight lines in the plotter outputs.

divided by the total number of free crossbridges: $f(K) = K3 \cdot Mp/(M + Mp)$. $g(K)$ was defined as the ratio of total flux of crossbridge detachment divided by the total number of attached crossbridges (as measured by isometric stress): $g(K) = (K4 \cdot AMp + K7 \cdot AM)/(AMp + AM)$.

To model crossbridge cycling in the negative force–bearing region, we assumed that g in the negative force–bearing region was proportional to the sum of cycling rate constants at $x = h$, as described by Huxley (17). That is, $g_2 = c(f_1 + g_1)$, where c is a constant. The rationale for this assumption was that crossbridge cycling rates at both positive and negative force–bearing x were proportional to the enzymatic activity of the myosin molecule. Using these equations to relate apparent cycling rate constants to strain-dependent crossbridge cycling rate constants, the coupled four-state model predicted the phosphorylation-dependent stress-velocity relationships (15); and the proportionality constant, c, was found to be 6.8 (15). In this study, we used the same proportionality and rate constants to calculate the model's prediction of ATP consumption during isometric and isotonic contractions and compared model predictions to experimental data.

The rate of actin-activated myosin ATP hydrolysis was computed by calculating the rate of crossbridges entering the crossbridge cycle for a given shortening velocity (v) and spacing (d) of crossbridge-binding sites along an actin filament. This was done by integrating crossbridge fluxes throughout the range of x:

$$\frac{v}{d}\int_{x=-\infty}^{x=+\infty} f(1-n)\,dt,$$

where n represented the fraction of crossbridge attachment at a given x and time (t), which could be calculated from the strain-dependent cycling rate constants (f and g), h, and v. Since velocity equals dx/dt, this integral was simplified to:

$$\frac{1}{d}\int_{-\infty}^{+\infty} f(1-n)\,dx \qquad (1)$$

The average rate of crossbridges entering the crossbridge cycle (Eq. 1) also equals J_{Cycle} because 1 mol of ATP is consumed per crossbridge cycle. This integral was used to compute all results in this study.

Isometric contraction

The integral given by Eq. 1 for calculating J_{Cycle} was solved by first calculating n as a function of x. For isometric contractions, n was constant and equaled $f_1/(f_1 + g_1)$ between $x = 0$ and $x = h$ and equaled 0 at other crossbridge positions (17). Therefore, Eq. 1 was simplified to:

$$\frac{1}{d}\int_0^h \frac{f_1 x}{h}\cdot\left(1-\frac{f_1}{f_1+g_1}\right)dx. \qquad (2)$$

This integral was solved analytically to calculate J_{Cycle} during isometric contraction, which equaled $hf_1g_1/[2d(f_1 + g_1)]$. Since $f_1 = 4f(K)$ and $g_1 = 4g(K)$, J_{Cycle}

also equaled $2hf(K)g(K)/d[f(K) + g(K)]$. We (15) previously assumed that h equaled 15.6 nm and d equaled the spacing between two actin monomers in a thin filament (5.9 nm; reference 22). The rationale for choosing these values has been discussed previously (15). Substituting the values of h and d into the equation, $J_{Cycle} = 5.3f(K)g(K)/[f(K) + g(K)]$. It is noteworthy that $f(K)g(K)/[f(K) + g(K)]$ is what the kinetic flux analysis predicts for J_{Cycle}. Therefore, J_{Cycle} predicted by coupling the four-state model with Huxley's approach was higher than that predicted by kinetic flux analysis (16, 19) by a factor of 5.3. As described by Eq. 2, the factor 5.3 was a product of the ratios $f_1/f(K)$, $g_1/g(K)$, and the relative dimension of h and d. These parameters were not considered previously in kinetic flux analysis (16, 19).

The factor 5.3 corrects J_{Cycle} but does not necessarily invalidate the original four-state model prediction (19) and the assumption used for the coupled model that crossbridge phosphorylation was faster than crossbridge cycling. This is because isometric stress produced by a muscle is supported by a population of crossbridges differing in position, force, and cycling rates, and the effective cycling rate of an average crossbridge is still described by the apparent cycling rate constants. The rate of myosin phosphorylation is faster than the rate of cycling of an average crossbridge in the swine carotid media because the rate constants for myosin phosphorylation are higher than the rate constants for isometric stress development (Fig. 1). Statistically, at a given time period, the probability for a unit of myosin to change its state of phosphorylation is higher than the probability for a unit of isometric force to change its state of force.

Therefore, according to Huxley's model of crossbridge cycling (17), the rate of isometric force development may underestimate the overall rate of actin-activated myosin ATP hydrolysis. Using Huxley's approach and estimates of h, d, and maximum v of swine carotid media, we calculated that the overall rate of ATP consumption by actin-activated myosin ATP hydrolysis was underestimated by a factor of 5.3. These calculations illustrate that crossbridge flux defined by rate of isometric stress development does not necessarily equal the overall rate of actin-activated myosin ATP hydrolysis. The assumption that crossbridge phosphorylation is faster than crossbridge cycling is less critical for calculating steady-state rates of ATP consumption described in this study. However, this assumption may be critical for calculating transient changes in ATP consumption rates when there are rapid changes in the number of attached crossbridges, such as during the early phase of an isometric contraction. If crossbridge phosphorylation is not faster than crossbridge cycling, then the four crossbridge states should be modeled separately as having individual phosphorylation- and strain-dependent crossbridge cycling rates.

The integral given by Eq. 2 was used to compute J_{Cycle} as a function of myosin phosphorylation. The increase in myosin phosphorylation was simulated by increasing the two rate constants (*K1* and *K6*) representing Ca^{2+}-dependent myosin light chain kinase activity. ATP consumption by myosin phosphorylation (J_{Phos}) was calculated from crossbridge fluxes along the pathways labeled by *K1* and *K6*. The model predicted that J_{Cycle} and J_{Phos} both had an almost linear dependence on myosin phosphorylation (Fig. 3). Furthermore, J_{Cycle} and J_{Phos} are comparable in magnitude for a given level of myosin phosphorylation.

The results shown in Fig. 3 could be used together with our earlier results on the dependence of isometric stress on myosin phosphorylation (10, 14) to compute the relationship between isometric stress and the total rate of ATP consumption ($J_{Total} = J_{Cycle} + J_{Phos}$) for comparison with experimental data. Previously the four-state model predicted the experimental observation that steady-state isometric stress had a quasi-hyperbolic dependence on myosin phosphorylation (14). Since J_{Total} had an almost linear dependence on myosin phosphorylation (Fig. 3, —), the model predicted that steady-state isometric stress had a quasihyperbolic dependence on J_{Total}.

This finding appeared to be inconsistent with the experimental observation that the relationship between isometric stress and suprabasal rate of ATP consumption was linear (5, 7, 21, 23). However, it is important to note that available steady-state data on smooth muscle energetics do not cover the full range of myosin phosphorylation. Typically, myosin phosphorylation was not

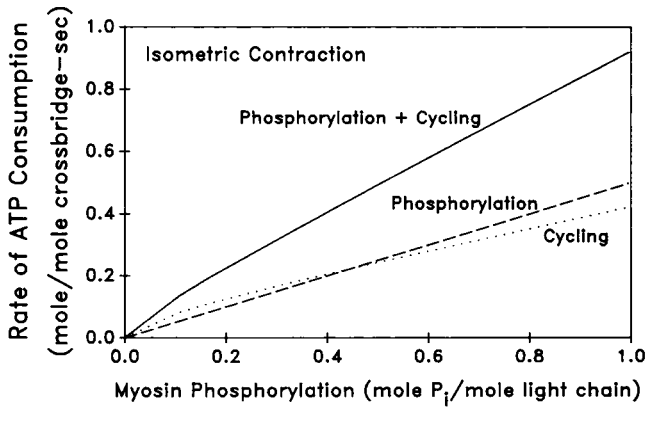

FIGURE 3 Predicted rates of ATP consumption during isometric contraction by crossbridge phosphorylation (– – –), crossbridge cycling (· · · ·), and phosphorylation + cycling (——) at myosin phosphorylation levels ranging from 0 to 96%.

measured in most studies of smooth muscle energetics, and was estimated to be only 30% during steady-state contraction in one study (24). Data on myosin phosphorylation are important because the predicted relationship between isometric stress and J_{Total} is approximately linear when myosin phosphorylation is $<35\%$. To determine whether the model predicted experimental data, we compared the model prediction directly with experimental data.

We chose the data sets published by Peterson and Glück (23) and Krisanda and Paul (24) for comparison with the model prediction, because the swine carotid media were used in these two studies for the measurement of ATP consumption, and by Singer and Murphy (25) for the measurement of isometric force and myosin phosphorylation during fast contractions induced by electrical stimulation. This was important because rate constants for the four-state model (Fig. 1) were derived primarily from the data set reported by Singer and Murphy (10, 25).

Isometric stress was expressed in gwt/cm^2 by Peterson and Glück (23) and in mN/mm^2 by Krisanda and Paul (24). For simplicity, the unit of Peterson and Glück's isometric stress data was converted to mN/mm^2 (1 gwt/cm^2 = 9.807×10^{-2} mN/mm^2). Next, it was necessary to convert the isometric stress unit in the model prediction (fraction of total crossbridges) to mN/mm^2 for quantitative comparison with these two data sets. Ratz et al. (14) measured the steady-state relationship between isometric stress myosin phosphorylation in the swine carotid media and estimated that maximum isometric stress generated by the swine carotid media at optimal length was 1.8×10^5 N/m^2 (or 180 mN/mm^2). Since we assumed a ratio of 4:1 (*K3*/*K4*) for the phosphorylated crossbridge cycle (Fig. 1), the maximum number of attached crossbridges would be 80% of the total number of crossbridges. Therefore, a 1% crossbridge attachment in the model prediction was equivalent to 2.25 mN/mm^2. It is important to emphasize that these values of 80% for maximum crossbridge attachment and 1.8×10^5 N/m^2 for maximum active stress were not chosen to fit the energetics data. These values were used previously to fit the kinetics of isometric stress development and the steady-state relationship between isometric stress and myosin phosphorylation. They were retained here for consistency.

Rates of ATP consumption were expressed as mole ATP/mole crossbridge per second in the model prediction and as micromole ATP/gram wet weight per minute in the experimental data by Peterson and Glück (23) and Krisanda and Paul (24). The unit conversion for ATP consumption required data on the total crossbridge content in the swine carotid media (in moles crossbridge/gram wet weight). Murphy et al. (26) reported an average myosin content of 13 mg/g wet wt in the swine carotid media, which was equivalent to 0.0277 μmol myosin/g wet wt, assuming a mol wt of 470 kD for the smooth muscle myosin (26). We (10) previously assumed that the two heads of myosin cycle independently. With this assumption, the total crossbridge content would be two times the total myosin content, or 0.0553 μmol crossbridge/g wet wt. The final conversion factor was that 1 mol ATP/mol crossbridge per s in the model prediction was equivalent to 3.32 μmol ATP/g wet wt per min. All of the values used in generating predictions were taken from the literature without adjustment to best fit the data.

Data from Peterson and Glück's graded $[Ca^{2+}]_0$ and $[K^+]_0$ experiments and the model prediction are illustrated in Fig. 4 *A*. The model predicts the data when isometric stress is <125 mN/mm^2 but does not fit the data at higher isometric stress. However, an unknown variable is the level of myosin phosphorylation in Peterson and Glück's (23) tissues at a given level of isometric stress. As discussed before, the model assumed a maximum isometric stress of 180 mN/mm^2 if all the crossbridges were phosphorylated. The level of steady-state myosin phosphorylation in K^+-depolarized arterial smooth muscle at physiological $[Ca^{2+}]_0$ has been measured in many laboratories. Murphy and co-workers (11, 14, 27–29) reported steady-state myosin phosphorylation value induced by K^+ depolarization in the swine carotid media of 0.20–0.25 mole inorganic phosphate/mole light chain (mol P_i/mol LC). This was consistent with Jiang and Morgan's (30) value of 0.20 mol P_i/mol LC in the ferret aorta, and Ishikawa et al.'s (31) report of 0.25 mole P_i/mole LC in the bovine aorta. An exception is Barron et al.'s (32) estimates of 0.70 mol P_i/mol LC for steady-state myosin phosphorylation induced by K^+ depolarization in the swine carotid media. The basal myosin phosphorylation in their experiments was also high (0.37 mol P_i/mol LC). The reason(s) for the difference is unknown, but an assumed value of 0.22 mol P_i/mol LC for steady-state myosin phosphorylation induced by K^+ depolarization is consistent with most data in the literature. Clearly, the predicted stress at 0.22 mol P_i/mol LC ($\sim$120 mN/mm^2, Fig. 4 *A*) is much lower than that measured by Peterson and Glück. Reported estimates of maximum stress for the swine carotid media vary from $\sim$150 to 300 mN/mm^2 in different studies (3, 14, 27, 29), depending on tissue preparation (viability factors), stimulation conditions (steady-state phosphorylation levels), values used for the wet/dry weight ratio used to calculate cross-sectional areas, and perhaps differences in cell fraction or other factors associated with obtaining arteries from animals of different ages, sexes, or strains (48).

A reasonably good fit to the data (Fig. 4 *A*, ▲) could

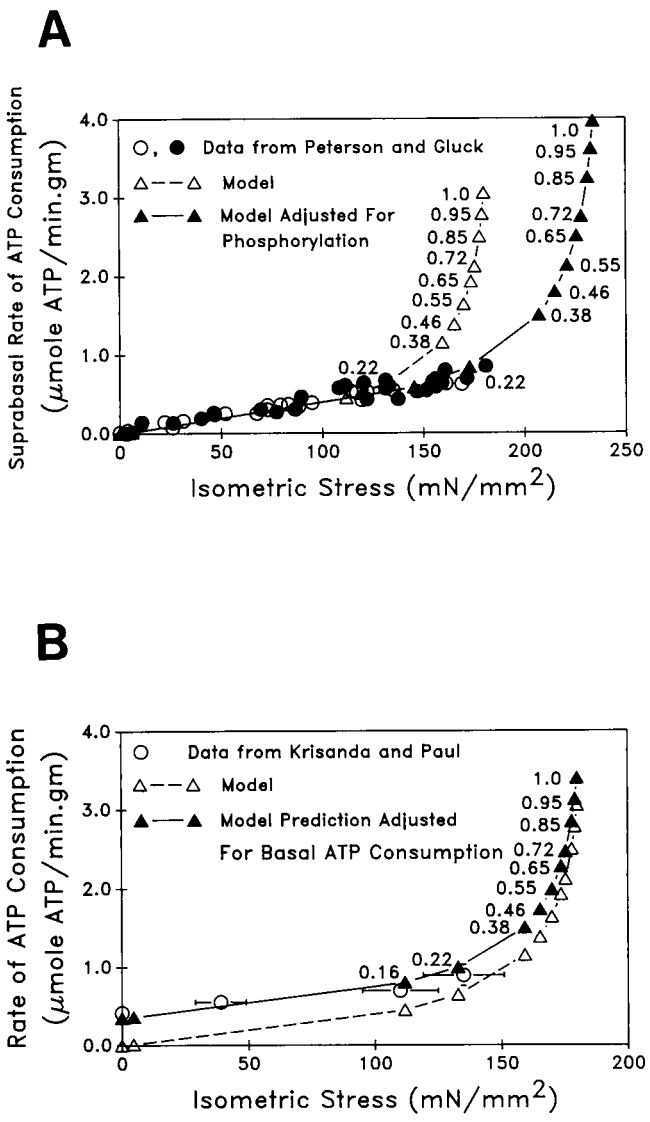

FIGURE 4 Comparison between model predictions △--△ and ▲——▲) and experimental data (○, ●) from (*A*) Peterson and Glück (○ and ● represent data from graded $[Ca^{2+}]_0$ and $[K^+]_0$ experiments, respectively, as published in reference 23), and (*B*) Krisanda and Paul (○; mean ± SE from reference 24) on the relationship between isometric stress and the rate of ATP consumption. In *A*, two model predictions are shown: assuming a maximum stress of 180 mN/mm² and myosin content of 13 mg/g wet wt (△--△) and assuming a maximum stress of 234 mN/mm² and a myosin content of 17 mg/g wet wt (▲——▲). In *B*, the model prediction is shown with (▲——▲) and without (△--△) adjustment for basal rate of ATP consumption (see text). Numerical values shown next to triangles represent the predicted levels of myosin phosphorylation (in mol P_i/mol LC) in the tissues.

be obtained if the maximum stress at 100% phosphorylation was assumed to be 234 (instead of 180) mN/mm², and the average myosin content was assumed to be 17 (instead of 13) mg/g wet wt in Peterson and Glück's tissues. The results indicate that the model can predict Peterson and Glück's data with adjusted parameters that are certainly well within the errors of experimental measurements. Clearly, a data set consisting of only the rates of ATP consumption and isometric stress is insufficient for definitive testing of the coupled four-state model. Additional data on myosin phosphorylation and myosin content in the same experimental study are needed for quantitative comparison with the model prediction.

The data reported by Krisanda and Paul (24) and the model prediction (converted to the same units) were plotted together in Fig. 4 *B* (○). The model prediction does not include the basal rate of ATP consumption at zero stress. Krisanda and Paul (24) measured the basal rate of ATP consumption at zero isometric stress by slacking the tissue and lowering $[Ca^{2+}]_0$ to 0.15 mM; they reported a value of 0.42 ± 0.06 μmol ATP/min per g wet wt. The model prediction, even with an assumed maximal stress of 180 mN/mm², fitted all data points within 1 SE, assuming 0.35 μmol/min per g wet wt as the basal rate of ATP consumption (Fig. 4 *B*).

The model fitted Krisanda and Paul's oxygen consumption data and predicted a myosin phosphorylation level of 0.22 mol P_i/mol LC at 7.5 mM $[Ca^{2+}]$. Krisanda and Paul followed the protocol described by Aksoy et al. (27) but did not measure myosin phosphorylation. At 7.5 mM Ca^{2+}, the level of myosin phosphorylation reported by Aksoy et al. (27) was 0.4 mol P_i/mol LC, which exceeds the model's prediction of 0.22 mol P_i/mol LC. This difference, if real, would again be minimized if the maximal stress generation is higher than the estimated 180 mN/mm². This uncertainty again highlights the importance of having a complete data set consisting of myosin phosphorylation, isometric stress, and ATP consumption rates for definitive testing.

Isotonic contraction

The integral given in Eq. 1 could also be used for computing J_{Cycle} during isotonic contractions. A major difference between computing model predictions for isometric and isotonic contractions was the distribution of attached crossbridges as a function of crossbridge position. During isometric contraction, crossbridges were distributed uniformly between $x = 0$ and $x = h$, as discussed before. During isotonic contractions, crossbridges were distributed unevenly throughout the negative ($x < 0$) and positive ($x > 0$) force-bearing positions. We first calculated n as a function of x for a given shortening velocity (V in optimal muscle lengths/second), contractile unit length (s), and h. We then solved Eq. 1 using n, $f(K)$, and $g(K)$ to compute J_{Cycle}

during isotonic contraction:

$$J_{Cycle} = \frac{2hf(K)}{d[f(K) + g(K)]}\left[g(K) + f(K)\frac{V}{\phi}(1 - e^{-\phi/V})\right],$$

where $\phi = 4h[f(K) + g(K)]/s$.

s was assumed to be 2.2 μm and the values of h and d were the same as defined before (15). The model predicted an increase in J_{Cycle} with muscle shortening (Fig. 5*A*). Since $f(K)$ and $g(K)$ were functions of individual rate constants (*K1–K7*), the model also predicted an increase in J_{Cycle} with myosin phosphorylation as a result of increases in *K1*, *K6* (Ca^{2+}-dependent myosin light chain kinase activity). We computed J_{Cycle} as a function of shortening velocity for three different levels of myosin phosphorylation (Fig. 5 *A*) corresponding to the three stress–velocity relationships we analyzed previously (15). The result at zero shortening velocity ($V/V_{max} = 0$ in Fig. 5 *A*) represented the predicted rate of ATP consumption during isometric contraction (Fig. 3). Model predictions were computed for isotonic shortening velocities only up to 50% of the maximum shortening velocity (V_{max}) because it was generally recognized that Huxley's model could not account for energetics data beyond this range of shortening velocity (33). New models have been proposed to account for the decrease in the rate of ATP consumption at higher shortening velocities (33–35) by including additional crossbridge states. However, the contractile unit structure and crossbridge states in smooth muscle are poorly understood, and only limited data are available on smooth muscle energetics. Therefore, we chose not to expand the number of crossbridge states and limited the comparison of model predictions to data obtained at shortening velocities < 0.5 V_{max} for any level of phosphorylation.

The model predicted that J_{Cycle} during an isotonic contraction at 0.5 V_{max} would be higher than that during an isometric concentration ($V/V_{max} = 0$) by 2.9-fold when myosin phosphorylation was 26%. The corresponding values at 37 and 50% phosphorylation were 3.4- and 3.9-fold, respectively. There were no quantitative data on shortening-induced increases in the rate of ATP consumption in arterial smooth muscle for comparison. However, some data were available on the rate of ATP consumption during muscle shortening in rabbit taenia coli. Butler et al. (36) observed shortening-induced increases in the rate of ATP consumption in rabbit taenia coli during the later steady-state phase of a contraction. The observed increase was 2.5-fold at 24–28% myosin phosphorylation, a value similar to the model prediction of a 2.8-fold increase at 26% myosin phosphorylation for the swine carotid media.

A major energetic difference between isometric and isotonic contractions is mechanical work output, which

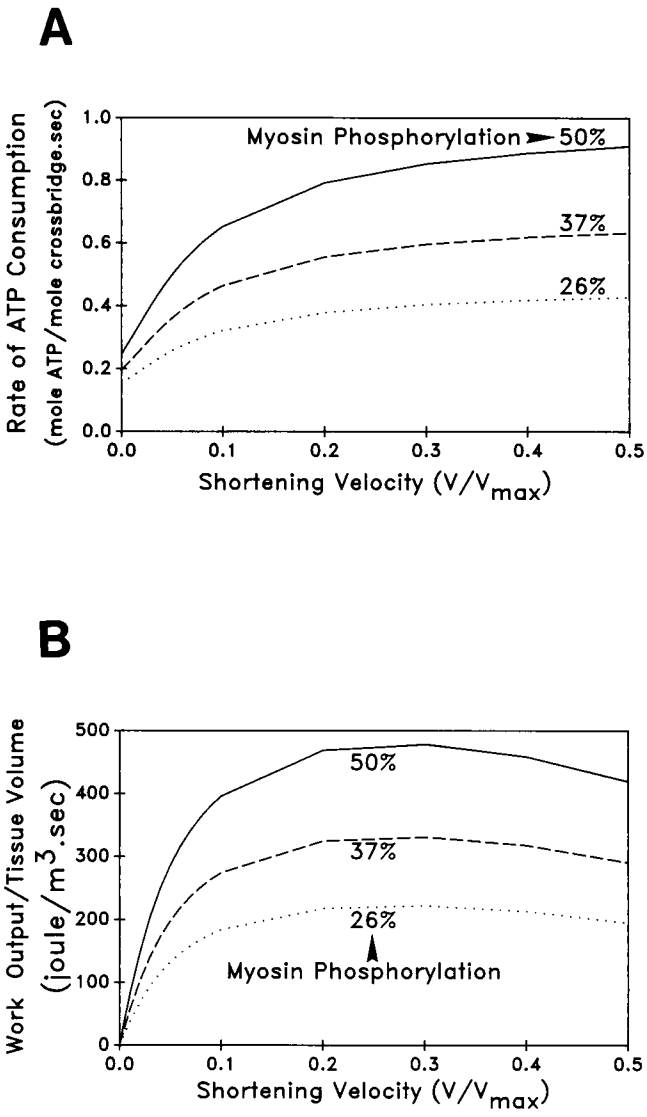

FIGURE 5 Model predictions of (*A*) rate of ATP consumption by crossbridge cycling and (*B*) rate of mechanical work output (or power) as functions of shortening velocity at 26, 37, and 50% myosin phosphorylation in the swine carotid media. The corresponding maximum shortening velocities were 0.026, 0.037, and 0.05 optimal length/s, respectively (4, 15). Shortening velocities (V) are normalized by the maximum shortening velocity (V_{max}) at a given level of myosin phosphorylation. Only results at shortening velocities between 0 and 50% V_{max} are shown (see text).

is zero in isometric contraction. A useful index of muscle efficiency is work output/mole ATP consumption during shortening. We first computed the mechanical work output predicted by the model and then calculated the ratio of work output/mol ATP using values of J_{Cycle} and J_{Phos} as calculated before. The product of stress (force/area) and normalized shortening velocity (in optimal muscle lengths/time) equaled mechanical work output/

tissue volume-s or power, as shown in the following analysis. Consider a muscle with cross-sectional area = A m^2 and optimal muscle length = L m, that generates a stress of S N/m^2 at a normalized shortening velocity of V muscle lengths/s. The total force generated by the muscle is therefore SA N, and the rate of movement is VL m/s. The total mechanical work done by the muscle per time is then $SAVL$ J/s. Since AL equals tissue volume, mechanical work done per time ($SAVL$) also equals SV × tissue volume (AL). In other words, the product SV (stress × normalized shortening velocity) equals mechanical work done per time per tissue volume.

We used the same conversion factor (2.25 mN/m^2 per 1% crossbridge attachment) described above to compute work output/time per tissue volume (in J/s per m^3) as a function of shortening velocity (Fig. 5 *B*). As expected from the hyperbolic stress–velocity relationship (3), work output was zero at zero shortening velocity (isometric contraction) and reached a maximum at ~30% of V_{max}. The predicted work output also increased with myosin phosphorylation (Fig. 5 *B*) as expected from the phosphorylation dependence of the stress–velocity relationship in smooth muscle (2, 4).

A relevant question was then whether the predicted increases in rates of work output and ATP consumption were proportional. That is, was the predicted work output/mol ATP phosphorylation dependent? This question was addressed by computing work output/mol ATP consumption by dividing work output/time per tissue volume (Fig. 5 *B*) by the sum of J_{Phos} (Fig. 3) and J_{Cycle} (Fig. 5 *A*) for a given shortening velocity. The same conversion factors (0.0277 μmol myosin/g wet wt and 2 crossbridges/myosin molecule) were used to convert the units of J_{Cycle} and J_{Phos} to mol ATP/s per g wet wt. A tissue density of 1.05 kg/liter for the swine carotid media (37) was used to convert the unit of J/s per m^3 to J/s per g wet wt. The final ratio therefore had the unit of J/mol ATP (Fig. 6). The model predicted that phosphorylation-dependent increases in the rates of work output and ATP consumption were almost proportional such that work output/mol ATP consumption (index of efficiency) was only slightly dependent on myosin phosphorylation (Fig. 6). For example, predicted maximum work output/mol ATP increased by only 5.4% (from 7.4 to 7.8 kJ/mol ATP) when myosin phosphorylation increased from 26 to 50%. The predicted work output/mol ATP consumption had a biphasic dependence on shortening velocity (Fig. 6). Maximum work output per ATP occurred at ~20% of V_{max}, which was lower than the shortening velocity associated with maximum work output (Fig. 5 *B*). Butler et al. (36) measured work output/mol ATP in the rabbit taenia coli and reported a value of 7.1 kJ/mol ATP, which was slightly lower than the predicted value of 7.4–7.8 kJ/mol ATP for the swine carotid media. This was expected because crossbridge phosphorylation and cycling are the only ATP-consuming processes in the model calculation.

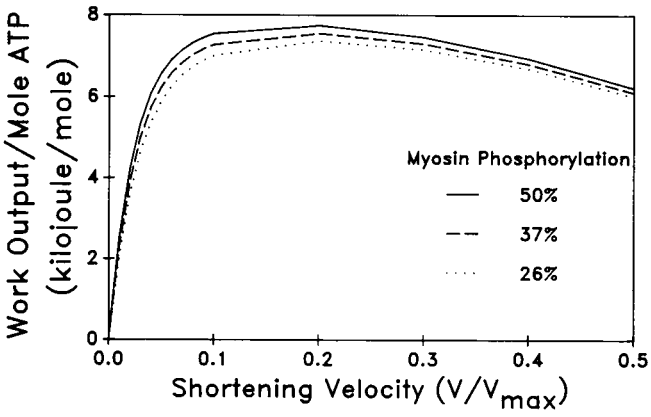

FIGURE 6 Predicted work output per mole ATP as a function of shortening velocity and myosin phosphorylation. Shortening velocity (V) is normalized by maximum shortening velocity (V_{max}). Relationships in this figure were calculated from results illustrated in Figs. 3 and 5 (see text). Crossbridge phosphorylation and cycling were assumed to be the only ATP-consuming processes in the calculation.

Overview of the four-state model

Since the publication of the four-state model (10), the following two questions have been raised.

Selection of the rate constants

Computer simulations were performed to show the effects of 10-fold increases or decreases in a given rate constant on model predictions of myosin phosphorylation and isometric stress during a 60-s contraction (Fig. 7). The original assumptions, that $K1 = K6$, $K2 = K5$, and $K3 = 4K4$, were retained. In each panel of Fig. 7, the solid line represents the original model prediction that fitted Singer and Murphy's data (25). Actual values of rate constants that were changed are shown in all panels of Fig. 7.

As expected, an increase in *K1*, *K6* (myosin light chain kinase activity) resulted in a higher level of myosin phosphorylation at any time greater than zero (Fig. 7*A*). An increase in *K1*, *K6* also resulted in a higher level of isometric stress at any time greater than zero (Fig. 7 *B*) because crossbridges must be phosphorylated before they could attach to the actin filament in the four-state model. Conversely, an increase in *K2*, *K5* (myosin light chain phosphatase activity) resulted in lower levels of myosin phosphorylation (Fig. 7 *C*) and isometric stress at any time greater than zero (Fig. 7 *D*). A 10-fold

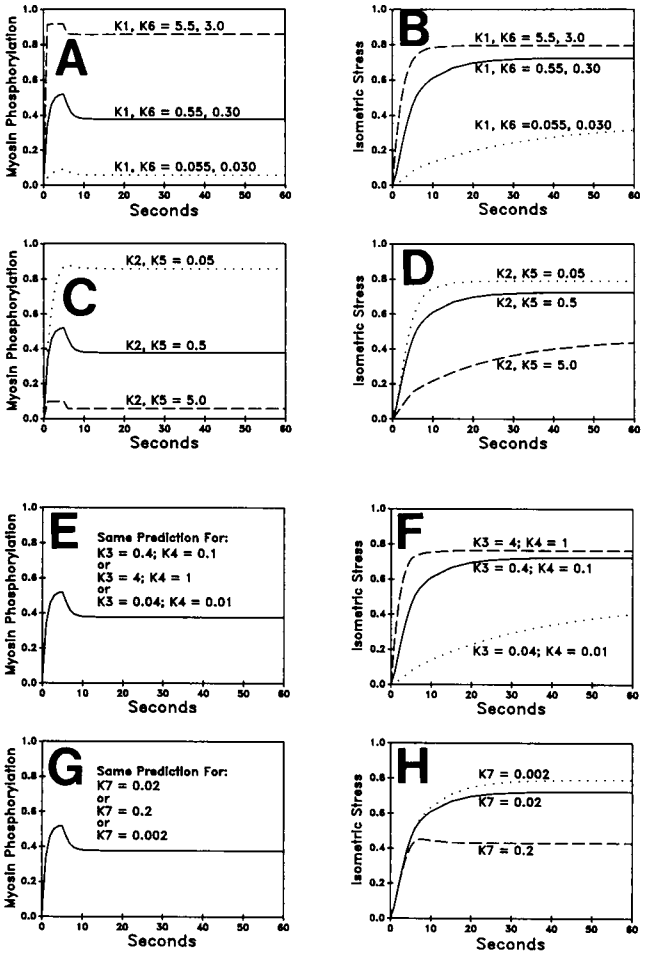

FIGURE 7 Effects of 10-fold increase (– – –) and 10-fold decrease (· · · · ·) of *K1*, *K6* (*A* and *B*); *K2*, *K5* (*C* and *D*); *K3* and *K4* (*E* and *F*); and *K7* (*G* and *H*) on model predictions of myosin phosphorylation (*A*, *C*, *E*, and *G*) and isometric stress (*B*, *D*, *F*, and *H*). Model predictions represented by solid lines were obtained by using the following set of rate constants (in s^{-1}): *K1*, *K6* = 0.55 (0–5 s of stimulation), 0.30 (5–60 s of stimulation); *K2*, *K5* = 0.5; *K3* = 0.4; *K4* = 0.1; and *K7* = 0.02.

increase in *K3* and *K4* (cycling rate constants of phosphorylated crossbridges) had no significant effect on myosin phosphorylation (Fig. 7 *E*) but resulted in higher isometric stress at any time greater than zero (Fig. 7 *F*). Similarly, a 10-fold increase in *K7* (rate constant for latchbridge detachment) had no effect on myosin phosphorylation (Fig. 7 *G*) but resulted in a lower isometric stress at times > 5 s (Fig. 7 *H*). The model predictions of myosin phosphorylation and isometric stress at different times of a contraction were selectively more sensitive to certain rate constants. This made it possible to resolve a self-consistent set of rate constants with the three stated assumptions that gave predictions within the SEs of the data points.

Irreversible latchbridge detachment

In the four-state model, *K7* described latchbridge detachment ($AM \rightarrow A + M$), but there was no rate constant describing the reverse reaction ($A + M \rightarrow AM$). Two questions were raised concerning this assumption: (*a*) whether this assumption was a violation of the principle of microscopic reversibility in chemical kinetics and (*b*) whether this assumption was inconsistent with the findings of Greene and Sellers (38) that myosin phosphorylation had no effect on the binding of heavy meromyosin.ADP to actin in vitro.

It is important to emphasize that this assumption is not meant to violate the principle of microscopic reversibility. It is meant to imply that the rate constant for attachment of free crossbridges to form force-generating units (*K8* for $A \rightarrow M$ to AM) was very small compared with *K7* (<0.01 *K7*) in smooth muscle cells. This assumption was analogous to the assumption that myosin phosphorylation catalyzed by myosin light chain kinase in vivo was essentially irreversible, although it was known that ATP could be synthesized by the reverse reaction catalyzed by myosin light chain kinase under appropriate experimental conditions (39). Mathematically, predictions of myosin phosphorylation and isometric stress by the four-state model with a very small *K8* or without *K8* were not significantly different. Table 1 lists the model predictions of myosin phosphorylation and isometric stress at 5 and 60 s after the beginning of a simulated smooth muscle contraction for different ratios of *K8*/*K7* ranging from 0 to 0.1. The rate constants *K1*–*K7* were the same as those fitted to Singer and Murphy's data. Inclusion of *K8* up to 10% of *K7* had no effect on the model prediction of myosin phosphorylation and affected the model prediction of stress at 5 and 60 s by <0.7 and 0.4%, respectively (Table 1).

Greene and Sellers (38) reported that myosin phosphorylation had no effect on the binding of heavy meromyo-

TABLE 1 Effect of *K8*/*K7* ratio on model predictions of myosin phosphorylation and isometric stress during a smooth muscle contraction

	Myosin phosphorylation		Isometric stress	
K8/*K7*	5 s	60 s	5 s	60 s
	mol P_i/mol LC		*fraction of total crossbridges*	
0	0.5211	0.3750	0.4544	0.7234
0.0001	0.5211	0.3750	0.4544	0.7234
0.001	0.5211	0.3750	0.4544	0.7235
0.01	0.5211	0.3750	0.4547	0.7237
0.1	0.5211	0.3750	0.4575	0.7262

Rate constants for these simulations were (in s^{-1}): *K1*, *K6* = 0.55 (0–5 s), 0.30 (5–60 s); *K2*, *K5* = 0.5; *K3* = 0.4; *K4* = 0.1; *K7* = 0.02. *K8* describes a possible $A + M \rightarrow AM$ reaction.

sin. ADP to actin. However, their results could not be extrapolated directly to crossbridge attachment in intact cells because changes in conformation induced by myosin phosphorylation could be more important than changes in binding affinity in intact cells. Trybus and Lowey (40) found that myosin light chain phosphorylation induced a conformational change of the smooth muscle myosin molecule from a folded form to an extended form. It is uncertain how this relates to the myofilament lattice where the tail of the myosin molecule is locked into the thick filament and the spacing between actin and myosin filaments is constrained. It is certainly reasonable to assume that unphosphorylated free crossbridges have very low probability of attachment in cells because both stiffness and isometric stress were low in resting tissues (41). These indexes of crossbridge attachment were even lower in Ca^{2+}-depleted tissues (41).

It is important to emphasize that attached crossbridges were defined functionally as strongly bound force-bearing and force-generating crossbridges. Weakly bound crossbridges such as A.M.ATP and A.M.ADP.P_i were equivalent to free crossbridges in a model constructed to predict the mechanical output of an intact smooth muscle. The possibility that some crossbridges could be strongly bound but non–force bearing was not supported by the findings of Singer et al. (41).

DISCUSSION

We proposed the four-state model as the simplest hypothesis that could explain many observations associated with contraction and the latch state in the swine carotid media (10, 13–15). However, the model's predictions of smooth muscle energetics have only recently been tested quantitatively against experimental data (16). In this study, we computed J_{Phos} and J_{Cycle} during isometric and isotonic contraction by coupling the four-state model with Huxley's concept (15, 17) of strain-dependent crossbridge cycling rates and compared model predictions with experimental data available for the swine carotid media.

A consistent finding in smooth muscle was a linear dependence of the rate of ATP consumption on isometric stress (5, 7, 21, 23). Paul (16) characterized this linear dependence as "... a hallmark of energetics in smooth muscle." Since the coupled four-state model did not predict a linear dependence of ATP consumption on isometric stress (Fig. 4), Paul (16) concluded that a "latch" model was inadequate and favored a model with a high ratio of *K3/K4* to explain the special energetics characteristics of smooth muscle. However, the apparently linear dependence of ATP consumption on stress might simply reflect the fact that steady-state phosphorylation levels in the swine carotid media rarely exceed 35% (a value that supports near maximal isometric stress) unless Ca^{2+} sequestering or extrusion mechanisms are inhibited experimentally (14). At the levels of phosphorylation elicited by most stimuli, the coupled four-state model predicts a virtually linear dependence of ATP consumption on steady-state stress. There are uncertainties in matching data sets from different laboratories, but the coupled four-state model can predict the energetics data obtained by Peterson and Glück (23) if the assumed stress generating capacity exceeds 220 mN/mm^2 and the results of Krisanda and Paul (24) on the swine carotid media (Fig. 4). These results lead to a testable hypothesis that the "hallmark of energetics of smooth muscle" is only an approximation, although it is valid in a statistical sense under physiological conditions. ATP consumption at high values of steady-state crossbridge phosphorylation must be measured to distinguish a linear from a nonlinear dependence of ATP consumption on stress.

J_{Cycle}, as calculated by the approach used in this study, was higher than our previous estimate using kinetic flux analysis (19) by a factor of 5.3. The factor 5.3 was a product of: (*a*) the relative dimensions of *h* and *d* and (*b*) the ratio of crossbridge cycling rate constants at *h* and the apparent cycling rate constants resolved from isometric force transients. These parameters were not considered in the kinetic flux analysis. The new approach used in this study is superior to the kinetic flux analysis (16, 19) because crossbridge cycling rates are generally considered to be strain dependent (20). Using the new approach, the predicted J_{Phos} and J_{Cycle} are comparable in magnitude, and both increase almost linearly with myosin phosphorylation in isometric contractions (Fig. 3). Therefore, the predicted ATP consumption by cycles of myosin phosphorylation and dephosphorylation was ~ 50% of total rate of ATP consumption under isometric conditions where the economy of force maintenance is very high (1). The predicted efficiency during shortening will also be much higher than the kinetic flux analysis suggested. Thus, this analysis removes or appreciably reduces objections to the coupled four-state model based on efficiency considerations (16).

Stress-independent ATP consumption has been measured by releasing a tissue until isometric stress was zero (slack length) and was found to be 20–30% of the total ATP consumption during steady-state contraction at optimal length (42, 43). This observation, with the implication that some 70–80% of the suprabasal ATP consumption was associated with crossbridge cycling, was interpreted as evidence that the coupled four-state model could not explain smooth muscle energetics (16). However, the assumption in these studies was that the

level of myosin phosphorylation was similar in tissues at slack and optimal length. Recently, Hai (28) measured myosin phosphorylation in swine carotid media at slack and optimal length under steady-state stimulation and found substantially lower levels of myosin phosphorylation in tissues at slack length. Furthermore, there was no significant difference in Ca^{2+}-activated phosphorylation levels in skinned tissues held at optimal and slack length (28). This was consistent with the findings of Moreland et al. (44) that Ca^{2+}-activated myosin phosphorylation was length insensitive in skinned swine carotid media. Therefore, the lower myosin phosphorylation in intact carotid media at slack length appeared to be due to reduced cytosolic $[Ca^{2+}]$. This was supported by the findings of Rembold and Murphy (29) that agonist-induced cytosolic $[Ca^{2+}]$ was reduced at 0.7 L_0 in the swine carotid media.

The predicted phosphorylation-dependent increases in the rates of work output and ATP consumption (Figs. 3 and 5) were expected because the apparent cycling rate constants were phosphorylation dependent and Huxley's model was known to predict a shortening-induced increase in ATP consumption. However, it was not intuitively obvious that the increase in work output was necessarily proportional to the increase in ATP consumption at a given shortening velocity. Therefore, it was unexpected that the predicted work output/mol ATP was relatively insensitive to myosin phosphorylation (Fig. 6). This is a specific model prediction that can be tested in future experiments.

The prediction of a phosphorylation-independent work output/mol ATP consumption was consistent with the findings of Butler et al. (45) on the taenia coli. Since shortening velocity was phosphorylation dependent, but efficiency of work production was relatively phosphorylation independent, Butler et al. (45) suggested that internal load was not important in the regulation of shortening velocity in smooth muscle. However, recent mechanical data from single smooth muscle cells reported by Harris and Warshaw (46) suggested that internal load was important in the regulation of shortening velocity in smooth muscle. The apparent contradiction between the energetics data and mechanics data might be reconciled by consideration of the dynamic exchange between latchbridges (AM) and cycling crossbridges (AMp) via myosin phosphorylation and dephosphorylation. Comparison of the detachment rates of latchbridges ($K7$ = 0.02) and phosphorylated crossbridges ($K4$ = 0.1) suggests that latchbridges (AM) could impose an internal load on the cycling crossbridges (AMp). However, two factors could reduce the effectiveness of a latchbridge (AM) as an internal load. First, a latchbridge (AM) could be converted to a cycling crossbridge (AMp) by phosphorylation. Second, crossbridge detachment rate at negative force-bearing positions may be very high $[g_2/(f_1 + g_1) = 6.8]$ in the swine carotid media (15), exceeding the value of 3.9 calculated for skeletal muscle (17).

Ca^{2+}-dependent activation of myosin light chain kinase and the coupled four-state model is one of many putative Ca^{2+}-dependent mechanisms proposed for the regulation of smooth muscle contraction and the latch state (10, 22, 47). However, this hypothesis is useful in its ability to provide specific predictions for experimental testing. The biophysical and energetics predictions are consistent with most of the available data in vascular smooth muscle. Still to be tested are the model's critical assumptions at the molecular level, such as whether attached crossbridges are substrates for myosin light chain kinase and myosin light chain phosphatase (10).

We especially thank Dr. Thomas M. Butler for his helpful comments on a draft of this manuscript.

This study was supported by grant DCB8902438 from the National Science Foundation (to C.-M. Hai) and grant 5 P01 HL-19242 from the National Institutes of Health (to R. A. Murphy).

Received for publication 8 August 1990 and in final form 10 October 1991.

REFERENCES

1. Murphy, R. A. 1988. The muscle cells of hollow organs. *News Physiol. Sci.* 3:124–128.
2. Aksoy, M. O., R. A. Murphy, and K. E. Kamm. 1982. Role of Ca^{2+} and myosin light chain phosphorylation in regulation of smooth muscle. *Am. J. Physiol.* 242(*Cell Physiol.* 11):C109–C116.
3. Dillon, P. F., M. O. Aksoy, S. P. Driska, and R. A. Murphy. 1981. Myosin phosphorylation and the cross bridge cycle in arterial smooth muscle. *Science Wash. DC* 211:495–497.
4. Dillon, P. F., and R. A. Murphy. 1982. Tonic force maintenance with reduced shortening velocity in arterial smooth muscle. *Am. J. Physiol.* 242(*Cell Physiol.* 11):C102–C108.
5. Arner, A., and P. Hellstrand. 1983. Activation of contraction and ATPase activity in intact and chemically skinned smooth muscle of rat portal vein. *Circ. Res.* 53:695–702.
6. Butler, T. M., and M. J. Siegman. 1985. High-energy phosphate metabolism in vascular smooth muscle. *Annu. Rev. Physiol.* 47:629–643.
7. Krisanda, J., and R. J. Paul. 1985. Energetics of isometric contraction in porcine carotid artery. *Am. J. Physiol.* 246(*Cell Physiol.* 15):C510–C519.
8. Siegman, M. J., T. M. Butler, S. U. Mooers, and R. E. Davis. 1980. Chemical energetics of force development, force maintenance, and relaxation in mammalian smooth muscle. *J. Gen. Physiol.* 76:609–629.
9. Walker, J. S., I. R. Wendt, and C. L. Gibbs. 1988. Heat production of rat anococcygeus muscle during isometric contraction. *Am. J. Physiol.* 255(*Cell Physiol.* 24):C536–C542.
10. Hai, C.-M., and R. A. Murphy. 1988. Cross-bridge phosphoryla-

tion and regulation of latch state in smooth muscle. *Am. J. Physiol.* 254(*Cell Physiol.* 23):C99–C106.

11. Hai, C.-M., and R. A. Murphy. 1989. Ca^{2+}, crossbridge phosphorylation, and contraction. *Annu. Rev. Physiol.* 51:285–298.
12. Kamm, K. E., and J. T. Stull. 1985. The function of myosin and myosin light chain phosphorylation in smooth muscle. *Annu. Rev. Pharmacol. Toxicol.* 25:593–620.
13. Hai, C.-M., and R. A. Murphy. 1989. Cross-bridge dephosphorylation and relaxation of vascular smooth muscle. *Am. J. Physiol.* 256(*Cell Physiol.* 25):C282–C287.
14. Ratz, P. H., C.-M. Hai, and R. A. Murphy. 1989. Dependence of stress on cross-bridge phosphorylation in vascular smooth muscle. *Am. J. Physiol.* 256(*Cell Physiol.* 25):C96–C100.
15. Hai, C.-M., and R. A. Murphy. 1988. Regulation of shortening velocity by cross-bridge phosphorylation in smooth muscle. *Am. J. Physiol.* 255(*Cell Physiol.* 24):C86–C94.
16. Paul, R. J. 1990. Smooth muscle energetics and theories of cross-bridge regulation. *Am. J. Physiol.* 258(*Cell Physiol.* 27):C369–C375.
17. Huxley, A. F. 1957. Muscle structure and theories of contraction. *Prog. Biophys. Mol. Biol.* 7:255–318.
18. More, J., B. Garbow, and K. Hillstrom. 1980. User Guide for MINPACK-1. Argonne, IL: Argonne National Laboratory, Report ANL-80-74.
19. Hai, C.-M., and R. A. Murphy. 1992. Crossbridge phosphorylation and the energetics of contraction in the swine carotid media. Proc. Third International Congr. Muscle Energetics, R. J. Paul, K. Yamada, and M. Elzinga, editors. Allan R. Liss, New York. In press.
20. Eisenberg, E., and T. L. Hill. 1985. Muscle contraction and free energy transduction in biological systems. *Science Wash. DC* 227:999–1006.
21. Arner, A., and P. Hellstrand. 1985. Effect of calcium and substrate on force-velocity relation and energy turnover in skinned smooth muscle of the guinea-pig. *J. Physiol. Lond.* 360:347–365.
22. Marston, S. B., and C. W. J. Smith. 1985. The thin filaments of smooth muscles. *J. Muscle Res. Cell Motil.* 6:669–708, 1985
23. Peterson, J. W., and E. Glück. 1982. Energy cost of membrane depolarization in hog carotid artery. *Circ. Res.* 50:839–847.
24. Krisanda, J. M., and R. J. Paul. 1988. Dependence of force, velocity, and O_2 consumption on $[Ca^{2+}]_0$ in porcine carotid artery. *Am. J. Physiol.* 255(*Cell Physiol.* 24):C393–C400.
25. Singer, H. A., and R. A. Murphy. 1987. Maximal rates of activation in electrically stimulated swine carotid media. *Circ. Res.* 60:438–445.
26. Murphy, R. A., J. T. Herlihy, and J. Megerman. 1974. Force-generating capacity and contractile protein content of arterial smooth muscle. *J. Gen. Physiol.* 64:691–705.
27. Aksoy, M. O., S. Mras, K. E. Kamm, and R. A. Murphy. 1983. Ca^{2+}, cAMP, and changes in myosin phosphorylation during contraction of smooth muscle. *Am. J. Physiol.* 245(*Cell Physiol.* 14):C255–C270.
28. Hai, C.-M. 1991. Length dependence of myosin phosphorylation and contraction of arterial smooth muscle. *Pfluegers Arch.* 418:564–571.
29. Rembold, C. M., and R. A. Muprhy. 1990. Muscle length, shortening myoplasmic $[Ca^{2+}]$, and activation of arterial smooth muscle. *Circ. Res.* 66:1354–1361.
30. Jiang, M. J., and K. G. Morgan. 1989. Agonist-specific myosin phosphorylation and intracellular calcium during isometric contractions of arterial smooth muscle. *Pfluegers Arch.* 413:637–643.
31. Ishikawa, T., T. Chijiwa, M. Hagiwara, S. Mamiya, M. Saitoh, and H. Hidaka. 1988. ML-9 inhibits the vascular contraction via the inhibition of myosin light chain phosphorylation. *Mol. Pharmacol.* 33:598–603.
32. Barron, J. T., K. Bàràny, M. Bàràny, and S. J. Kopp. 1989. Effects of ATP reduction on the pattern of force development and myosin light chain phosphorylation in intact arterial smooth muscle. *Biochim. Biophys. Acta.* 1010:278–282.
33. Woledge, R. C., N. A. Curtin, and E. Homsher. 1985. Energetic Aspects of Muscle Contraction. Academic Press, London.
34. Huxley, A. F., and R. M. Simmons. 1971. Proposed mechanisms of force generation in striated muscle. *Nature Lond.* 233:533–538.
35. Podolsky, R. J., and A. C. Nolan. 1973. Muscle contraction transients, cross-bridge kinetics, and the Fenn effect. *Cold Spring Harbor Symp. Quant. Biol.* 37:661–668.
36. Butler, T. M., M. J. Siegman, and S. U. Mooers. 1983. Chemical energy usage during shortening and work production in mammalian smooth muscle. *Am. J. Physiol.* 244(*Cell Physiol.* 13):C234–C242.
37. Herlihy, J. T., and R. A. Murphy. 1973. Length-tension relationship of smooth muscle of the hog carotid artery. *Circ. Res.* 33:275–283.
38. Greene, L. E., and J. R. Sellers. 1987. Effect of phosphorylation on the binding of smooth muscle heavy meromyosin.ADP to actin. *J. Biol. Chem.* 262:4177–4181.
39. Ikebe, M., and D. J. Hartshorne. 1986. Reverse reaction of smooth muscle myosin light chain kinase. *J. Biol. Chem.* 261:8249–8253.
40. Trybus, K. M., and S. Lowey. 1984. Conformational states of smooth muscle myosin. *J. Biol. Chem.* 259:8564–8571.
41. Singer, H. A., K. E. Kamm, and R. A. Murphy. 1986. Estimates of activation in arterial smooth muscle. *Am. J. Physiol.* 251(*Cell Physiol.* 20):C465–C473.
42. Paul, R. J., Glück, E., and J. C. Rüegg. 1976. Cross bridge ATP utilization in arterial smooth muscle. *Pfluegers Arch.* 361:297–299.
43. Paul, R. J., J. D. Strauss, and J. M. Krisanda. 1987. The effects of calcium on smooth muscle mechanics and energetics. *In* Regulation and Contraction of Smooth Muscle. M. J. Siegman, A. P. Somlyo, and N. L. Stephens, editors. Alan R. Liss, New York. 319–332.
44. Moreland, R. S., S. Moreland, and R. A. Murphy. 1988. Dependence of stress on length, Ca^{2+}, and myosin phosphorylation in skinned smooth muscle. *Am. J. Physiol.* 255(*Cell Physiol.* 24): C473–C478.
45. Butler, T. M., and M. J. Siegman, and S. U. Mooers. 1986. Slowing of cross-bridge cycling in smooth muscle without evidence of an internal load. *Am. J. Physiol.* 251(*Cell Physiol.* 20):C945–C950.
46. Harris, D. E., and D. M. Warshaw. 1990. Slowing of velocity during isotonic shortening in single isolated smooth muscle cells. *J. Gen. Physiol.* 96:581–601.
47. Kamm, K. E., and J. T. Stull. 1989. Regulation of smooth muscle contractile elements by second messengers. *Annu. Rev. Physiol.* 51:299–313.
48. Sparrow, M. P., and H. W. Mitchell. 1990. Contraction of smooth muscle of pig airway tissues from before birth to maturity. *J. Appl. Physiol.* 68:468–477.